#21: Performance analysis of thermochemical energy storage integrated with heat pump for building applications

Norhayati MAT WAJID[1], Abdul Murad ZAINAL ABIDIN[1] Omer SIDDIG[2], Saffa RIFFAT[2]

[1] Energy Efficiency and Renewable Energy Expert Division, Mechanical Engineering Branch, Public Works Department of Malaysia, Menara Kerja Raya, 50480, Kuala Lumpur, Malaysia. NorhayatiMat.jkr@1govuc.gov.my
abdmurad.jkr@1govuc.gov.my

[2]Institute of Sustainable Energy, Department of Architecture and Built Environment, University of Nottingham, NG7 2RD, Nottingham, UK. saffa.riffat@nottingham.ac.uk
siddig.omer@nottingham.ac.uk

The aim of this study is to evaluate the performance during the adsorption and desorption process of a thermochemical energy storage (TES) system integrated with a heat-pump circuit. The chemical reactions of TES produce low-temperature heat, which is then transferred into the room or closed piping system to reduce the room temperature of a building. The low temperature will be used as alternative air-conditioning and will be eliminated or reduce the energy of using the conventional systems that consume high electricity. Furthermore, during the desorption process by using a heat pump, it will be operated during the off-peak hours which the rate of electricity much lower compared to peak hours. In this study, a numerical model was used to determine the regeneration temperature and TES performance. The numerical analysis was carried out using two different cycles; an adsorption cycle and desorption cycle. The operating temperature used in the modelling for charging is 60°C and the discharging is 50°C. In governing the equations on describing the thermal performance of TES, the basic refrigerant circuit of a vapour compression system was used for the adsorption heat pump. From the material synthesising and selection for this study, the material was chosen for this numerical modelling is vermiculite+$CaCl_2$.The Engineering Equation Solver (EES) is used for the modelling of regeneration via heat pumps. The modelling was carried using two (2) different type of refrigerant in the heat pump which was the R134a and R1234yf. TES has a higher COP when using R134a compared to R1234yf ranges from 1.44 to 1.98 and 0.33 to 0.48 when the heating temperature is increasing. Other than that, the mass variation change the COP of TES using R134a has higher COP compared to TES using R1234yf ranges from 0.042 to 2.75 and 0.006 to 1.05. However, the desorption time has effect adverse on the COP, the COP of TES of using R134a is lower compared to TES of using R 1234yf ranges from 0.92 to 0.03 and 9.4 to 0.05.

Keywords: energy storage; heat pump; performance; building applications

1. INTRODUCTION

The purpose of this paper is to study the theoretical adsorption and desorption process of a thermochemical heat storage system (TES) when integrated with an electric heat clamp, a heat-pump circuit, and using solar energy. A numerical model was used to determine the regeneration temperature and TES performance. The numerical analysis was carried out using two different cycles; an adsorption cycle and a desorption cycle. In governing the equations on describing the thermal performance of THSS, the basic refrigerant circuit of a vapour compression system was used for the adsorption heat pump. This is because the regeneration process is similar to the vapour compression systems which use the R134A (TES-R134a) and R1234yf (TES-R1234yf) as the refrigerant gas. These refrigerant gases were selected based on previous literature aimed towards investigating adoption of low global-warming potential gases for the proposed systems. Furthermore, it has been reported by Zilio, Brown et al. (2011) and Lee and Jung (2012) that R1234yf has four global warming potential (GWP) and zero ozone depletion potential (ODP) compared to the conventional R134a which is 1430 GW (BOC 2019). In this study, both refrigerants were modelled on the desorption process to investigate their effect on the performance of the TES. For the adsorption process, the heat of adsorption is calculated using the adsorption equilibrium which is dependent on the pressure and temperature as in accordance with the Linear Driving Force Method (Aristov, Tokarev et al. 2006, El-Sharkawy, Abdel Meguid et al. 2014) .From the material synthesising and selection for this study, the material was chosen for this numerical modelling is vermiculite+$CaCl_2$. These composite material was selected due to the high adsorption temperature. At the end of the modelling process, the performance of TES was discussed, and the conclusion was drawn by comparing the three adsorption methods.

2. METHODOLOGY

The TES cycle is similar to the basic heat pump cycle in that it consists of two main operational phases, namely adsorption and desorption. The regeneration phase occurs during night hours, when cheap electricity is available under the 'Economy 7' that is more suitable for households with night storage heaters or that use lots of electricity at night. For the electric heating element this model draws on a concept whereby the household use the electric boiler. For the heat pump circuit, the model suggests using a heat pump as the desorption method for the heat storage system for residential. Using solar energy as the heat source may not influence the tariff change. The physical details of the TES-R134a/R1234yf system is illustrated in Figure 1. As the compressor starts to operate, the heat from the refrigerant will desorb the water vapour into the adsorbent pipe and then flow through the evaporator pipe. The latent heat is reversible, and water vapour is stored as a liquid in the adsorbent pipe.

2.1. Modelling of transport of heat and adsorbate

The computer modelling for transport of heat and adsorbate is based on the principle of the adsorption heat pipe coupled with the analytical method developed using EES programme. Vermiculite, impregnated with $CaCl_2$, was selected to predict the performance of TES. The assumptions on governing the heat balance equation are according to previous modelling (Miyazaki, Akisawa et al. 2009, Zhang, Wang et al. 2011) as listed below:

i) The temperatures of the adsorbent and adsorbate are assumed to be the same at all times.
ii) A lump parameter approach is used in the present study to describe the energy and heat balance equations for each element of the adsorption systems.
iii) The pressure difference between the condenser and the evaporator was neglected.
iv) The refrigerant adsorbed uniformly in the adsorber and was liquid in the adsorbent.

2.2. Adsorption isotherm

The numerical values in calculating this adsorption isotherm is based on the previous model developed by (Miyazaki, Akisawa et al. 2009).

$$q^* = A(Ts)\left[\frac{P_S(T_w)}{P_S(T_S)}\right]^{B(T_S)} \quad (1)$$

Where

Numerical value for A

$$A(T_S) = A_0 + A_1T_S + A_2T^2{}_S + A_3T^3{}_S \quad (2)$$

Numerical value for B

$$B(T_S) = B_0 + B_1T_S + B_2T^2{}_S + B_3T^3{}_S \quad (3)$$

The numerical values of $A_0 - A_3$ and $B_0 - B_3$ are provided in Table 1.

Table 1: Value of Parameter used for the adsorption isotherm (Miyazaki, Akisawa et al. 2009)

Parameter	Value
A_0	-6.5314
A_1	0.072452
A_2	-0.23951×10^{-3}
A_3	0.25493×10^{-3}
B_0	-15.587
B_1	0.15915
B_2	-0.50612×10^{-3}
B_3	0.5329×10^{-6}

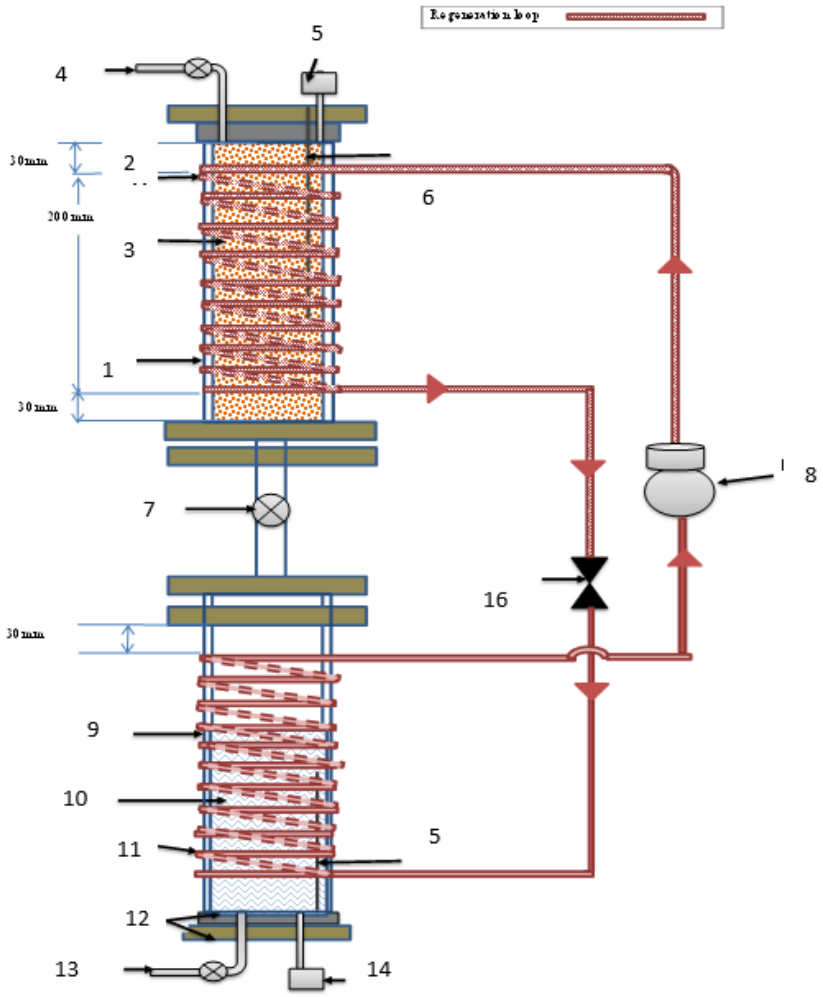

Figure 1: Schematic of TES-R134a/TES-R1234yf

Table 2: Descriptions of THSS-R134a/1234yf

No	Description	Size
	Condenser Section	
	Pipe Type	Cylindrical Borosilicate Glass
1	Condenser Pipe	QVF glass, ID 50mm, maximum pressure 4 bar_g, maximum temperature :200°C , heat transfer area: 448 cm^2, thermal conductivity (λ: 1.2 W/m.K), Density (ρ): 2.23 kg/dm^3, specific heat (cp): 0.8 KJ/kg.K
2	Coil pipe	¼" diameter coil
3	Adsorbent material	50gram Vermiculite +$CaCl_2$
4	Valve to vacuum pump	ball valve
5	Pressure sensor	GP pressure transmitter
6	Thermocouple	RTD thermocouple
7	Separation valve	Swagelok ball valve
8	Compressor	miniature DC inverter compressor (ZH2024, Greatcool) displacement of 1.5cm^3/rev, input power of 220W
	Evaporator Section	
	Pipe type	Cylindrical borosilicate Glass
9	Evaporator Pipe	QVF glass, ID 50mm, maximum pressure 4 barg, maximum temperature :200° C , heat transfer area: 448 cm^2, thermal conductivity (λ: 1.2 W/m.K), Density (ρ): 2.23 kg/dm^3, specific heat (cp): 0.8 KJ/kg.K
10	Water	100 grams
11	Coil	¼" diameter copper tube coil
12	Flanges	Swagelok flange 50 mm diameter
13	Valve to vacuum pump	Ball valve
14	Pressure sensor	GP pressure transmitter
15	Thermocouple	RTD thermocouple
16	Expansion valve	R134a expansion valve

2.3. Adsorption rate

The adsorption rate for the present study is estimated according to (Miyazaki, Akisawa et al. 2009) use of the Linear Driving Force Method (LDF) in equation (4) below.

$$\frac{dq}{dt} = k_s a_v (q^* - q) \quad (4)$$

Where, q^* is the possible equilibrium amount that adsorbs, for this study its numerical value will be 0.55 based on the experimental results from the vertical adsorbent pipe. $k_s a_v$ is the overall mass transfer coefficient of the adsorbent or refrigerant pair and can be written as:

$$k_s a_v = \frac{15 D_S}{R_P^2} \quad (5)$$

Where, R_p is the adsorbent particle radius and D_S is the surface diffusivity and can be expressed by an Arrhenius equation as shown below:

$$D_s = D_{so} \exp\left(-\frac{E_a}{RT}\right) \quad (6)$$

Where, D_{so} is the pre-exponential term, E_a is the activation energy of surface diffusion. One of the most important conditions for using Equation 6 is that D_s must be constant (Tien, 1994) The value of D_{so} and E_a were reported as 2.54 x10-4 m2/s and 4.2 x104 J/mol respectively (Sakoda & Suzuki,1986).

2.4. Mass balance of adsorbate

In this study water is used as the adsorbate. Since the quantity of water which exists in the gas phase is negligible in comparison with those in other phases, the mass balance of adsorbate (water) is described as follows (Sakoda and Suzuki 1986)

$$M_s \frac{dq}{dt} + \frac{dM_w}{dt} = 0 \quad (7)$$

Where M_s is the weight of adsorbent in the adsorbent bed, M_w is that of water in the evaporator and t is time.

2.5. Heat balance in the adsorption cycle

During the adsorption cycle, the movement of heat in the adsorption cycles was considered. Figures 2 & 3 illustrate the vapour transport during the adsorption process. The heat balance of the adsorption pipe and that of adsorbent particles can be expressed as:

$$\frac{d}{dt}\left(C_s M_s T_s\right) = Qst \cdot M_S \cdot \frac{d_q}{d_t} - h_{stp} \cdot A_{stp} \cdot \left(T_s - T_p\right) \quad (8)$$

The left part of the model is the heat from the adsorption process through the adsorbent material. The first term from the right provides the heat generated due to the condensation of the desorbed water, while the second term provides the heat rejected to the reactor pipe. The isosteric heat of adsorption Qst, is thermodynamically derived from the adsorption equilibrium given in Equation 1. Due to the difficulty of the theoretical description of these phenomena and also for the simplification of this model, Qst was considered constant in this study as 2.8 MJ/kg, which was given in the literature by (Sakoda and Suzuki 1986),

For an adsorbent pipe with heat rejection to ambient, the temperature of the pipe is determined by;

$$\frac{d}{dt}\left(C_s M_s T_s\right) = h_{stp} \cdot A_{stp} \cdot \left(T_s - T_p\right) - h_a \cdot A_a \cdot \left(T_p - T_a\right) \quad (9)$$

Where C_s, M_s, T_s is the heat capacity, the mass and temperature of the adsorbent material respectively, and T_p is the temperature of adsorbent pipe, h_{stp}, A_{stp} are the heat transfer coefficient and area between the adsorbent bed and the adsorbent pipe wall, and h_a and A_a are the heat transfer coefficient of the atmosphere and area between the atmosphere and adsorbent pipe wall. For this study, the Euler method is used for solving the numerical integration to determine the temperature of the adsorbent and evaporator pipe according to (Nellis and Sanford 1990).

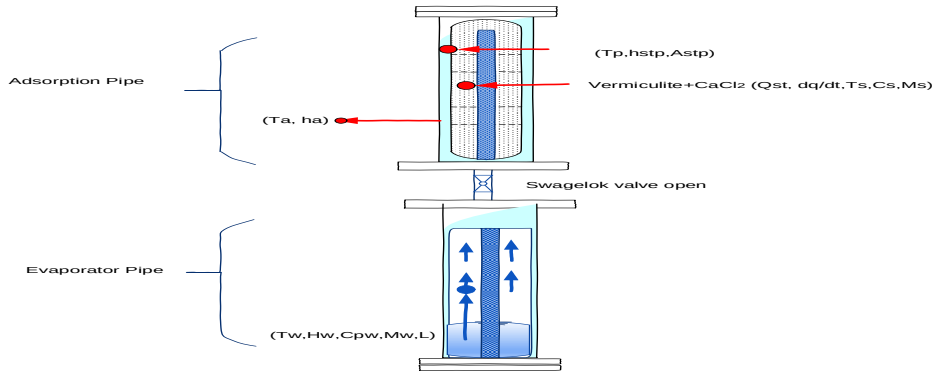

Figure 2: Heat transport of TES during adsorption.

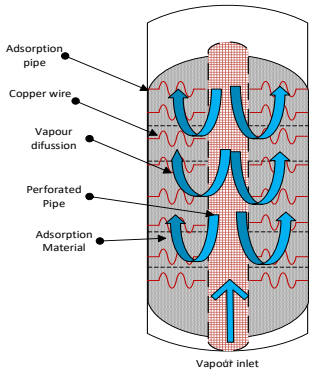

The average temperature of water in the evaporator pipe can be determined by:

$$\frac{d}{dt}(C_w M_w T_w) = h_w \cdot A_w \cdot (T_w - T_a) - L \cdot M_S \cdot \frac{d_q}{d_t} \quad (10)$$

Right hand side of the equation denote the heat from the evaporator and the left hand side denote the heat transfer from water to ambient. L is the latent heat of evaporation that is assumed to be equal to Qst (isosteric heat adsorption). It is necessary to calculate the heat transfer in the water tank, and thus h_w is determined by some experiments as the temperature drop of a typical water tank. The results showed that the effective heat transfer coefficient h_w is in the range of 400 - 600 W/m²K (Riffat, Su et al. 2013).

Figure 3: Detail of vapour diffusion in the adsorption pipe.

Parameters adopted in the simulation

The parameters used in this model can be divided into three categories (Table 3) which consist of adsorption properties, the design condition, and operation condition respectively. The adsorbent particles in the adsorbent bed were assumed to transfer only through the heat transfer glass wall. Its corresponding heat transfer area A_{stp} was regarded as the total surface area of the glass pipe and the heat transfer coefficient, h_{stp} , was estimated by using the following equation as the approximation (Sakoda and Suzuki 1986):

$$h_{stp} = \frac{k_e}{d/2} \quad (11)$$

Where d is the average distance between the heat transfer copper wire and k_e is the effective thermal conductivity of the packed bed, which was estimated at 1.35 W/m²K by (Tanashev, Krainov et al. 2013). The heat transfer coefficient between the ambient air and the container of the adsorbents (h_a), is taken as 1.23 W/m²K, which is often used as a similar empirical value for composite materials (Miyazaki et al., 2009). The parameter for vermiculite + $CaCl_2$ is difficult to find in the previous literature. Therefore, some assumptions must be used for this modelling. The activation energy (E_a) for vermiculite+$CaCl_2$ was estimated based on experiments of the dehydration of vermiculite studied by R.Sh.Mikhail et al. (1970) with a reading of 3.7kcal/mole (15 kJ/mole). The isosteric heat adsorption (Qst) estimation was based on a previous study done by Aristov et al. (2000), with a reading of 39.4kJ/mole.

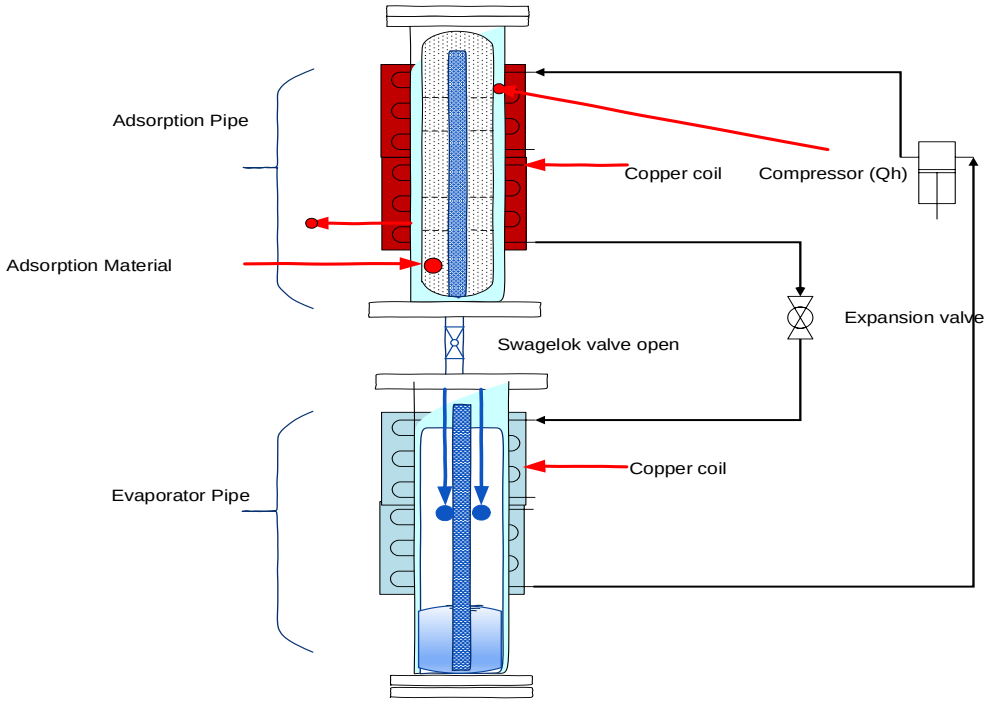

Figure 4: Heat transport of THSS-R134a/R1234yf

Table 3: Simulation physical Data for selected TES material

	Symbols	TES :Vermiculite + $CaCl_2$ (VCC)	Units
Adsorption Properties	$q\infty$ (water uptake)	0.55	kg/kg
	Dso (pre-exponential term)	2.54 x 10^{-4}	m^2/s
	Ea (activation energy)	1.5 x 10^4	J/mol
	Qst (isosteric heat of adsorption)	3940	kJ/kg
	M_b (Mass of adsorbent pipe)	0.75	kg
	M_s (Mass of adsorbent material)	0.05	kg
	M_w (Mass of water)	0.1	kg
	M_e (mass of evaporator pipe)	0.90	kg
Physical Properties	Length (L)	0.26	m
	Internal Diameter	0.05	m
	Outside Diameter	0.055	m
	Adsorbent bed Cartridge (empty)	0.67	kg
	Copper pipe	25	Nos turns
	Fins Spacing	0.01	m
	A_{stp} (Area of adsorbent cartridge)	0.045	m^2
	A_a(Area of adsorbent pipe)	0.047	m^2
	A_w (Area of water cartridge)	0.045	m^2
	h_a(Heat transfer coefficient between adsorbent pipe and ambient)	1.23	W/m^2K
	h_w(Heat transfer coefficient in evaporator (water cartridge)	400	W/m^2K
	R_p (adsorbent particle radius)	2.0 x 10^{-3}	m
	Cp (specific heat)	3.06 (Aydin et al., 2015a)	kJ/kgK
Operating Conditions	T_a (ambient temperature)	10	° C
	$T_{in,ads}$ (initial temperature in adsorbent pipe)	20	° C
	$T_{in,w}$ (initial temperature in water pipe)	17	° C
	T_s (adsorbent material temperature)	60	° C
	T_{fsolar} (solar collector final temperature)	80	° C

Movement of heat in the desorption cycle was similarly considered, as shown in Figure 4.

$$\frac{d}{dt}\left(C_{cp}M_{cp}T_{cp}\right) = Q_{st}Ms\frac{dq}{dt} - [h_a \cdot A_a \cdot \left(T_{cp} - T_a\right)] + Q_H \quad (12)$$

Where RHS denotes the heat in the adsorption pipe, and the first term of LHS is the adsorption heat and heat transfer from the adsorption pipe to ambient. Q_H is the heat from the heat pump as:

$$Q_H = \dot{m}(h_2 - h_3) \quad (13)$$

This equation is based on the heat pump Carnot cycle, where h_2 is the enthalpy from the refrigerant discharge temperature, h_3 is the enthalpy at the condenser temperature and $\dot{m}$ is the mass flow rate of refrigerant.

The compressor model

The compressor under consideration is a hermetic constant speed compressor, and the mass of refrigerant pumped and circulated by the compressor is given as (Mempouo 2011)

$$\dot{m} = \eta_v \cdot \frac{V_d \eta_v}{V_1} \quad (14)$$

The pumped mass of the refrigerant by the compressor can also be expressed in terms of the rotary speed (N) of the compressor as follows:

$$\dot{m} = \eta_v \cdot \frac{N V_d \eta_v}{60 v_1} \quad (15)$$

Where V_d is the displacement volume rate, η_v the volumetric efficiency of the compressor, and v_1 the specific volume at the inlet of the compressor.

The displacement volume (V_d) for a reciprocating-type compressor can be expressed as:

$$V_d = \frac{S_c \pi D_b^2}{4\ x\ 60} \quad (16)$$

The indicated power for compression can also be calculated in terms of the change of the enthalpy of the refrigerant from the inlet $h_1$to outlet h_2 of the compressor as follows:

$$W_{comp} = W_{oi} * \eta_{comp} = \dot{m}_r(h_1 - h_{2)} \quad (1712)$$

Where W_{oi} is the total ideal input electric power to the compressor, and η_{comp} is the general efficiency of the compressor.

The expansion valves model

The throttling process is regarded as the isenthalpic process. The mass flow rate is calculated as follows:

$$\dot{m}_r = k_{ex}\sqrt{2\rho_{in}(p_c - p_{ev})} \quad (18)$$

Where, k_{ex} is a proportionality constant and is changed as required to maintain the mix of gas and liquid in the evaporator and p_c and p_e are the condensing and evaporating pressures (Pa) respectively. The thermostatic expansion valve is modelled as an orifice through which the liquid is expanded from condensing to evaporating pressures. The mass flow rate through it can be correlated according to the Bernoulli equation (Fu, 2014):

$$\dot{m}_r = C_d A\sqrt{2\rho_{in}(p_c - p_{ev})} \quad (19)$$

Where ρ_{in} is the density of the refrigerant (liquid) at the inlet of the valve (kg/m^3), and A is the minimum flow area across the orifice. C_d is the flow coefficient, which depends upon the aperture of the valve. The maximum value is reached when the valve is fully open. C_d is evaluated through the empirical equation (Fu, 2014):

$$C_d = 0.02\sqrt{\rho_{in}} + 0.63v_{out} \quad (20)$$

Where v_{out} is the specific volume output of refrigerant.

The adsorbent pipe model/condenser coils

During the regeneration/charging process, the heat from the condenser coils will be transferred to the walls of the adsorbent pipe. The heat in the condenser coils can be determined by the following equation:

$$Q_H = \dot{m}(h_{2-} h_3) \quad (21)$$

Where $\dot{m}$ is the mass flow rate of the refrigerant (m^3/s), h_2 is the enthalpy heat refrigerant from the discharge pipe of the compressor (kJ/kg), and h_3 is the enthalpy of refrigerant from the outlet of the condenser coils of the system. The enthalpy heat is determined via thermo-physical properties libraries available in the EES software.

The evaporator coils

The heat from the evaporator coils transferred to the evaporator pipe walls can be determined by:

$$Q_e = \dot{m}(h_1 - h_4) \quad (22)$$

Where $\dot{m}$ is the mass flow rate of the refrigerant flow in the evaporator (m^3/s), h_1 is the enthalpy heat from the outlet of the evaporator coils to the compressor (suction) (kJ/kg), and h_4 is the enthalpy heat from the outlet of the expansion valve to the evaporator coils (kJ/kg).

2.6. System performance equation

The system performance of this small prototype was simplified as;

i. COP of the systems via electrical clamp for desorption

$$COP_1 = \frac{Q_{ads}}{Q_{electric}} \quad (23)$$

ii. COP of the systems via heat pump circuit for desorption

$$COP_2 = \frac{Q_{ads}}{Q_h} \quad (24)$$

iii. COP of the heat pump circuit

$$COP_{hp} = \frac{Q_h}{W_c} \quad (25)$$

2.7. Numerical result and discussion

Adsorption process

In this section, the results and discussion are mainly focused on the adsorption process of the TCM materials and their behaviours under the influence of change in saturation pressure (Ps) and adsorption uptake (dq/dt).

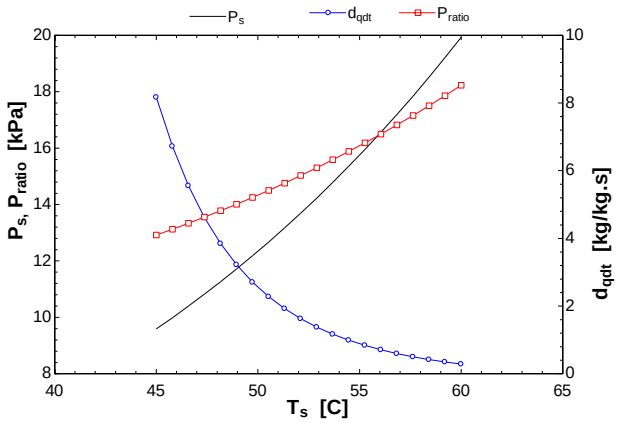

Figure 5: The effect of adsorption temperature vs. adsorption uptake and saturation pressure and pressure ratio.

Figure 5 exhibits the effect of increasing the adsorption material temperature (Ts) on saturation pressure and adsorption rate (dq/dt). As can be seen from these results, the increase in the adsorption temperature will decrease the adsorption uptake from 8.5kg/kg to 0.28kg/kg. However, the saturation pressure rises from 9kPa to 20kPa. These results suggest that the increase in adsorption temperature will increase the pressure ratio from 9kPa to 20kPa and the adsorption rate will decrease from 8kg/kg to 0.25kg/kg. This is because the reaction will take place during the adsorption cycle when the water vapour is absorbed by the adsorbent material. Therefore, it could be predicted that the adsorbent material temperature will be increased by the increase in adsorption rate during this period.

Desorption performance of TES using a heat-pump circuit with R134a as refrigerant gas

An analysis has been conducted on the performance of the TES during desorption by using a heat-pump circuit incorporated with the refrigerant gas of R134a. Three possible influential parameters that may affect the TES performance are: the heating temperature effect, the mass of material effect, desorption time effect, have been investigated and discussed below.

Heating temperature effect

Figure 6 shows the effect of heating temperature (TH) (R134a) on the adsorption heat and the compressor work. With the assumption of using constant dry mass of TES materials at 50g with 60g of water, the compressor work increases in a positive correlation with the heating temperature. However, the adsorption is expected to be constant throughout the desorption process as no reaction will occur. The heating temperature would also affect the COP system and the COP the heat pump. With the assumption of an ambient temperature (Ta) of 10°C, it would be expected that the COPhp would decrease from 6.15 to1.33 with the increase in heating temperature rising from 30-60°C, whereas it is expected the COP_2 would rise from 1.44 to 1.98. It can be predicted that as the heating temperature increases, the hydrated composite material will reach semi-equilibrium and lower energy levels will be required to disassociate the water vapour.

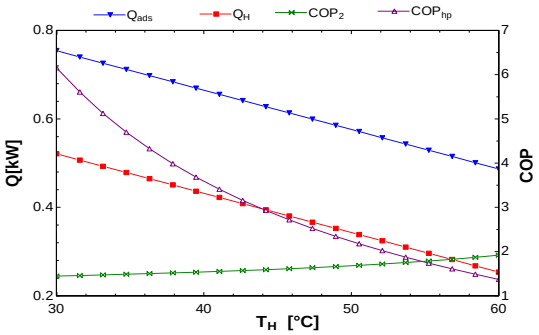

Figure 6: Adsorption heat, condenser heat, COP_2 and COP_{HP} vs. heating temperature (TES-R134a).

Mass of material effect

Figure 7 illustrates the effect of mass adsorbent material effect and predicted that with the assumptions of a heating temperature (TH) of 60°C and an ambient temperature (Ta) of 10°C, the heat pump heating power (Q_H) and the COP of the heat pump will remain constant at 0.026kW and 1.41 respectively. However, the adsorbent heat (Q_{ads}) and COP of the systems increased from 0.27 to 17kW and 0.042 to 2.75 respectively.

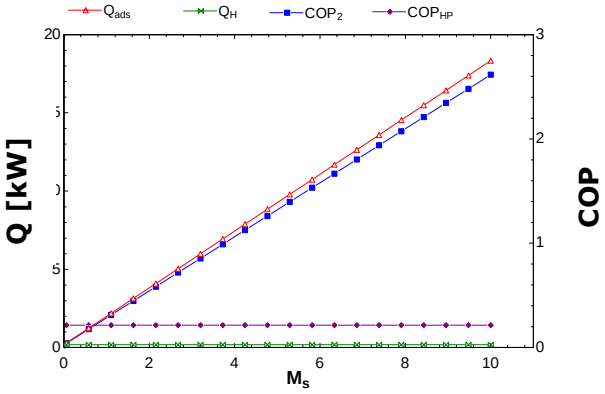

Figure 7: Effect of mass variation to heating power and the COP of the heat pump

Desorption time effect

Time dependence during desorption will also have an effect on the COP_{hp} and COP_2 as shown in Figure 8. With the assumption of the mass of Vermiculite Calcium Chloride at 0.05kg, the mass of water at 0.06kg, and with a heat source temperature of 60°C, the COP of the systems (COP_2) and COP of the heat pump (COP_{hp}) decreased from 0.92 to 0.03 and 1.4 to 0.02 respectively. In this case, the COP of the systems is higher than the COP of the heat pump. Furthermore, the adsorption heat (Qads) decreased from 0.233kW to 0.009kW; as time passed the heat will have been lost to the immediate environment.

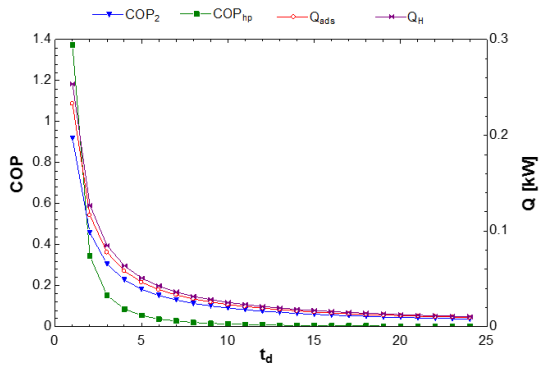

Figure 8: Effect of time on adsorption heat (COP_2) and the COP of the heat pump (R134a).

Desorption Performance of VCC using a Heat-Pump Circuit with R1234yf as the Refrigerant Gas

In this section, an analysis has been conducted on the performance of the TES during desorption using a heat-pump circuit incorporated with the refrigerant gas of R1234yf. Three possibly influential parameters that will affect the TES performance are the heating temperature effect, the mass of material effect and the desorption time effect, all of which have been investigated and discussed below.

Heating Temperature Effect

Figure 9 shows the effect of the heating temperature (TH) (R1234yf) on adsorption heat, heat pump heat, the COP of the heat pump (COPhp), and the COP of the system (COP_2). We can see that the effect of this on the COPhp is a decrease from 2.66 to 0.93, whereas the COP_2 has increased from 0.32 to 0.48. A higher COPhp compared to the lower COP_2 is due to the small amount of TES materials using lower heating power than was estimated to be required for the desorption process.

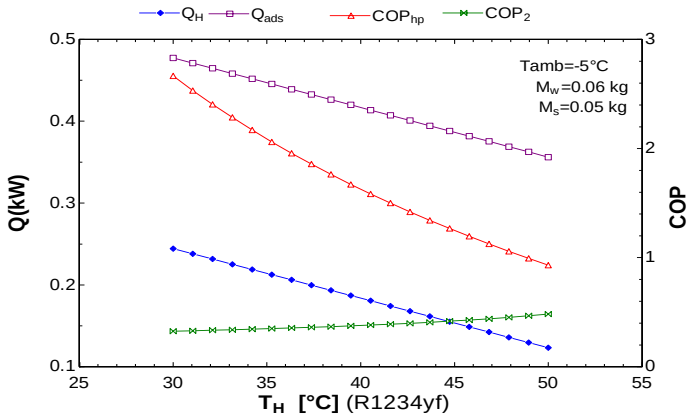

Figure 9: Effect of heating temperature on adsorption heat and compressor work.

Mass of Composite Adsorbent Effect

The increase of the TES material mass will increase the adsorption heat due to the increase of potential energy to be extracted from this material. Therefore, as can be seen in Figure 10 with the mass increase, the adsorbent heat (Q_{ads}) and the COP of the systems increase between the ranges of 0.28 to 46.6kW and 0.006 to 1.05 respectively. The COP of the heat pump (COP_{HP}) and the condenser heat (Q_H) remain constant because it is assumed that the heating temperature (T_H) and ambient temperature (T_a) are constant. However, during desorption, no reaction occurs. Therefore, we can only use this result to compare the effect of a mass increase in the systems quantitatively. However, we predict that if the mass of adsorbent material increases, it will increase the heating power that is required for disassociating the water vapour from the adsorbent material.

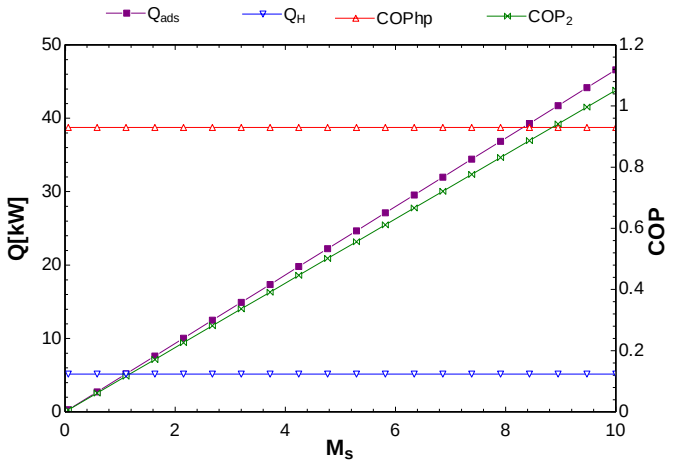

Figure 10: Effect of mass variation on adsorption heat and COP_2.

Desorption Time Effect

Time dependence will also have an effect on the COP_{hp} and COP_2 as shown in Figure 11. With the assumption that the mass of the VCC is 0.05kg and the mass of water is 0.06kg, the COP of the systems (COP_2) and the COP of the heat pump (COP_{hp}) are decrease from 9.4 to 0.005 and 0.92 to 0.08 respectively. From this result we can see that the COP of the systems is higher than that of the heat pump. The adsorption heat (Q_{ads}) and the condenser heat (Q_H) have decreased because as time passes the heat is lost to the immediate environment.

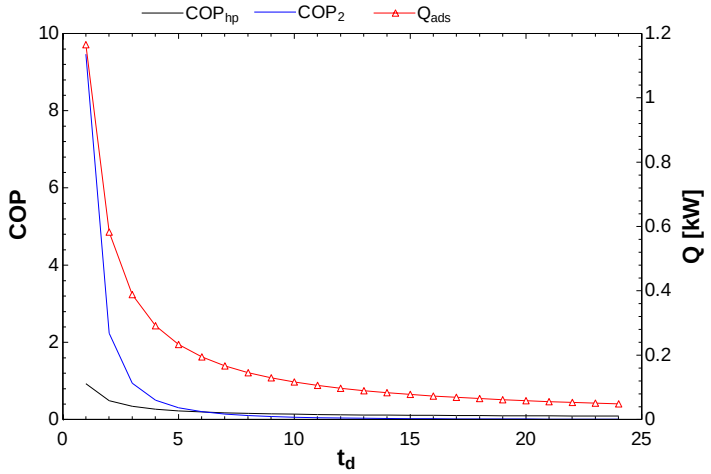

Figure 11: Effect of time on COP_2 and COP_{hp}.

Table 4: Summary results of all COP from the numerical analysis

Influence Factors	**Changing Rate**	**COP**	
		R134a	**R1234yf**
		COP_2	**COP_2**
Heating temperature	30-60°C	1.44 to 1.98	0.33 to 0.48
Mass Variation	2-10kg	0.042 to 2.75	0.006 to 1.05
Desorption time	1-24hr	0.92 to 0.03	9.4 to 0.05

3. CONCLUSION

Table 4 summarises the result of COP for all desorption heat source. It can be seen that the increase in heating temperature will increase the COP of the TES system. According to product/power theory, we predicted that the higher power input would have an adverse effect on the COP. Therefore, the decrease in COP when the heating temperature was increased was due to the small amount of mass (0.05kg) applied in the simulation and thus less energy was required for the desorption process. TES has a higher COP when using R134a compared to R1234yf ranges from 1.44 to 1.98 and 0.33 to 0.48 when the heating temperature is increasing. Other than that, the mass variation change the COP of TES using R134a has higher COP compared to TES using R1234yf ranges from 0.042 to 2.75 and 0.006 to 1.05. However, the desorption time has effect adverse on the COP, the COP of TES of using R134a is lower compared to TES of using R 1234yf ranges from 0.92 to 0.03 and 9.4 to 0.05.

4. REFERENCES

Aristov, Y. I., M. M. Tokarev, A. Freni, I. S. Glaznev and G. Restuccia (2006). "Kinetics of water adsorption on silica Fuji Davison RD." Microporous and Mesoporous Materials 96(1-3): 65-71.

BOC. (2019). "Opteon-R1234yf-Brochure410_124745.pdf." Retrieved 17/6/2019, 2019.

El-Sharkawy, I. I., H. Abdel Meguid and B. B. Saha (2014). "Potential application of solar powered adsorption cooling systems in the Middle East." Applied Energy 126: 235-245.

Fu, Y. (2014). Investigation Of Solar Assisted Heat Pump High-rise Residential Buildings., University of Nottingham, UK.

Lee, Y. and D. Jung (2012). "A brief performance comparison of R1234yf and R134a in a bench tester for automobile applications." Applied Thermal Engineering 35: 240-242.

Mempouo, B. (2011). Mempouo - 2011 - Investigations of Novel Heat Pump Systems for Low Carbon Homes.pdf, University of Nottingham, UK.

Miyazaki, T., A. Akisawa, B. B. Saha, I. I. El-Sharkawy and A. Chakraborty (2009). "A new cycle time allocation for enhancing the performance of two-bed adsorption chillers." International Journal of Refrigeration 32(5): 846-853.

Nellis, G. and K. Sanford (1990). Heat Transfer. United States of America.

Riffat, S., Y. Su and Y. Ding (2013). "Thermochemical cooling system based on adsorption pumping pipe." International Journal of Low-Carbon Technologies: ctt055.

Sakoda, A. and M. Suzuki (1986). "Simultaneous Transport of Heat and Adsorbate in Closed Type Adsorption Cooling System Utilizing Solar Heat." Journal of Solar Energy Engineering 108(239).

Tanashev, Y. Y., A. V. Krainov and Y. I. Aristov (2013). "Thermal conductivity of composite sorbents “salt in porous matrix” for heat storage and transformation." Applied Thermal Engineering 61(2): 401-407.

Tien, C. (1994). Adsorption Calculations and Modelling. USA, Butterworth-Heinemann.

Zhang, G., D. C. Wang, J. P. Zhang, Y. P. Han and W. Sun (2011). "Simulation of operating characteristics of the silica gel–water adsorption chiller powered by solar energy." Solar Energy 85(7): 1469-1478.

Zilio, C., J. S. Brown, G. Schiochet and A. Cavallini (2011). "The refrigerant R1234yf in air conditioning systems." Energy 36(10): 6110-6120.